International Micro Air Vehicle Conference and Flight Competition (IMAV2013)
17-20 September 2013, Toulouse, France

MAV Unsteady Characteristics in-Flight Measurement with the Help of SmartAP Autopilot

S. Serokhvostov, N. Pushchin and K. Shilov

Moscow Institute of Physics and Technology
Department of Aeromechanics and Flight Engineering
140180, Gagarina street, 16, Zhukovsky, Russia
serokhvostov@phystech.edu

Abstract

Proposed is the method of measuring the unsteady characteristics of Micro Air Vehicles (MAV) in flight with the help of small autopilot. Theoretical background, experimental methodic and results obtained are presented. Comparison with theoretical results is made.

1 Introduction

Unsteady characteristics of micro air vehicles (MAVs) can strongly affect on its flight performance (stability, controllability etc.). But up to now there was only the investigations of such characteristics for rather large airplanes. The characteristics for small ones can differ from those because of rather small values of Reynolds numbers and aircraft inertia characteristics. But the knowledge of these characteristics is important for the MAV design. So, it is required to check if the formulas for large aircrafts are applicable for small ones or we need to correct these formulas.

Some difficulties occur for the measurement of these characteristics in the wind tunnel. There must be special devices for model movements and rather precision measurement devices.

The another method of determination can be the flight test. To obtain the necessary data one must measure kinematical flight parameters (speed, rotation frequency, orientation of aircraft) and derive the unsteady characteristics.

One of the ideas of this investigation is to use autopilot system as a flight parameters recorder. The second idea is to separate the influence of inertia parameters (mass, inertia momentum) and the influence of aerodynamical effects. This can be made by changing the mass and changing the mass distribution in the aircraft. Using this technology one can analyze the influence of mass and center of gravity position, inertia momentums on the flight characteristics.

2 Experimental Equipment

2.1 Registration device

The main idea for the flight parameters registration is to use the small-sized autopilot. Indeed, the autopilot has all the sensors required and have many other useful features. Among the autopilots available the SmartAP autopilot [3], [1] was chosen, see fig. 1. The main features of this device are:

- light weight, it enables to use this device in rather small air vehicles;
- powerful microcontroller, which can give an opportunity to run routines at high frequencies;

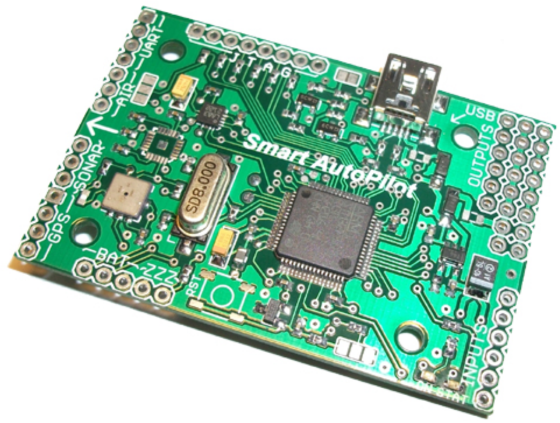

Figure 1: SmartAP autopilot

- 9-Degrees Of Freedom inertial measurement unit, which includes 3-axis accelerometer, 3-axis gyroscope and 3-axis magnetometer in order to determine attitude;
- pressure sensor for altitude measurement;
- differential pressure sensor for air speed measurement;
- GPS receiver for global position determination;
- wireless data channel for two-way telemetry;
- SD-card for in-flight data logging;
- USB port for PC/Laptop connection for firmware uploading, debugging and testing routines;
- PWM inputs/outputs to read signals from standard RC receiver and send them to motors/servos;
- Several ADC channels for battery voltage/amperage monitoring.

On the first stage it was decided to control the aircraft manually and collect the flight data and control signals on SD-card onboard. But it should be mentioned that this autopilot enables to make the measurements in fully automatic mode, i.e. the autopilot can guide the aircraft along the flight path, then make some disturbance, write the aircraft reaction to the SD-card and then correct the flight path.

Therefore, SmartAP autopilot is installed in-between standard RC receiver and servos. It provides the capability to register both pilot's input data and aircraft's behavior in form of linear accelerations, angular rates, Euler angles and airspeed measured by differential pressure sensor (Pitot tube). The logging frequency chosen is 50 Hz. Acceleration's measurement range was set to ± 4 g, gyroscopes range was set to ± 2000 deg/s.

2.2 Aircraft

As an experimental airplane the "Progress" model aircraft [4] was chosen (see fig. 2). The main characteristics of this plane are: mass — 150 gram; wingspan — 85 sm; wing aspect ratio — 3.9; wing

Figure 2: “Progress” model airplane with autopilot

taper ratio — 2.16; wing area — 0.82 m^2; horizontal tail surface — 0.053 m^2; horizontal tail distance from CG — 0.47 m; vertical tail surface — 0.0428 m^2; vertical tail distance from CG — 0.47 m.

This aircraft has rather low mass for this wing area, so the inertial effects in unsteady motion (including rotational ones) are much more less than the damping aerodynamic effects. This enables to investigate more easy the unsteady aerodynamical derivatives.

3 Theoretical Background

3.1 Conceptual Questions

The equations of disturbed motion form the system of 8 differential equations [2] that is very difficult or impossible for analytical research. One of the ideas for the analysis simplification was [2] to divide the motion on longitudinal and lateral.

The assumptions for the separation of the disturbed motion on lateral and transversal are [2]:

1. disturbances are small enough,

2. aircraft flies along the straight line without acceleration, without bank and slip,
3. air density is constant (flight altitude change is small enough),
4. aircraft is symmetrical along the vertical plane.

Also it follows from above assumptions that the aircraft must fly at the regimes without flow separation (as separation makes flow asymmetrical).

No more assumptions about the aircraft size and design and the Reynolds and Stroughal numbers and other parameters of similarity have not been made. So, as a conclusion, one can analyze the lateral and transversal motions of MAVs separately at least at rather important case of straight flight without acceleration and without flow separation.

So, at this stage of investigation the flight regimes were limited by the case of level flight with constant velocity.

3.2 Longitudinal Motion

Longitudinal disturbed motion (in Russian tradition) is usually analyzed in the coordinate system where OX axis is collinear to the velocity vector of aircraft, OY axis is perpendicular to OX and lies in the plane of aircraft symmetry and OZ axis is along the right semi-wing.

The values of characteristic scale of time

$$\tau = \frac{2m}{\rho S V_0},$$

and dimensionless aircraft density

$$\mu = \frac{2m}{\rho S L},$$

are required for further investigation (m is mass of MAV, ρ — air density, S — wing area, V_0 — non-disturbed flight velocity, L — wing span).

Let's make the following assumptions.

1. Mach number M is zero and all the coefficient's derivatives with respect to M are equal to zero.
2. Thrust vector is directed along the OX axis and is passed through the aircraft center of gravity.
3. Flight altitude is constant.

Under these assumptions the disturbed motion is described by the system of four non-dimensional linearized equations [2]. The solution of this system is in the form of $A\exp(\lambda t/\tau)$, where A is defined by initial conditions and λ is obtained from characteristical equation

$$\lambda^4 + a_1\lambda^3 + a_2\lambda^2 + a_3\lambda + a_4 = 0.$$

In common case λ is complex value. If the real part of λ is negative, then the disturbed motion is damped. This case is required for the stability conditions.

Coefficients of the characteristical equation can be found from formulas [2]

$$\begin{cases} a_1 &=& C_L^\alpha + 3C_D - \dfrac{m_z^{\omega z} + m_z^{\dot\alpha}}{r_z^2} - \dfrac{2T^V V_0}{\rho V_0 S}, \\ a_2 &=& -\dfrac{\mu m_z^\alpha + C_L^\alpha m_z^{\omega z}}{r_z^2} - \dfrac{m_z^{\omega z} + m_z^\alpha}{r_z^2}\left(2C_D - \dfrac{2T^V V_0}{\rho V_0^2 S}\right) + \\ & & +2\left(C_L^2 + (C_L^\alpha + C_D)\left(C_D - \dfrac{T^V V_0}{\rho V_0^2 S}\right) - C_L C_D^\alpha\right), \\ a_3 &=& -2\left(C_L^2 + (C_L^\alpha + C_D)\left(C_D - \dfrac{T^V V_0}{\rho V_0^2 S}\right) - C_L C_D^\alpha\right)\dfrac{m_z^{\omega z}}{r_z^2} - \\ & & -2C_L^2 \dfrac{m_z^{\dot\alpha}}{r_z^2} - 2\left(C_D - \dfrac{T^V V_0}{\rho V_0^2 S}\right)\dfrac{\mu m_z^\alpha}{r_z^2}, \\ a_4 &=& -2C_L^2 \dfrac{m_z^\alpha}{r_z^2}, \end{cases}$$

where $r_z^2 = I_{ZZ}/(mb^2)$ is dimensionless MAV radius of inertia for OZ axis, I_{ZZ} — aircraft moment of inertia about an axis OZ, b — mean wing chord, C_L — lift force coefficient, C_D — drag force coefficient, C_i^j — force coefficient derivatives with respect to some variable j, m_z^j — moment coefficient derivatives with respect to some variable j, α — angle of attack, ω_z — rotational frequency about an axis OZ, T^V — thrust derivative with respect to V.

The criteria for the stability of motion are
$a1 > 0$, $a2 > 0$, $a3 > 0$, $a4 > 0$, $R = a_1 a_2 a_3 - a_1^2 a_4 + a_3^2 > 0$.

The requirement $a_4 > 0$ assumes that $m_z^\alpha < 0$. This condition can be easily achieved by proper position of the center of gravity (forward of the aerodynamic center (AC)).

For the electrical powerplant $2T^V/(\rho V_0 S)$ is negative and of order of $(-C_D)$. So, the condition $a_1 > 0$ is certainly valid if $m_z^{\dot\alpha} < 0$ (for the most of cases $m_z^{\omega z} < 0$).

With the help of formulas from [2] it was found that $C_L \approx 0.5$, $C_D \approx 0.06$, $C_{D0} < 0.03$, $m_z^{\omega z} + m_z^{\dot\alpha} \approx$ ≈ -5.7 for horizontal tail, $m_z^{\omega z} \approx 0.3$ for the wing, $C_L \approx 3.6$, $\mu \approx 1.7$, $r_z \approx 0.7$, $m_z^\alpha \approx -0.18$, $\mu = 1.7$. For these values the coefficients a_2 and a_3 are positive. Also the above assumptions can help to simplify the expressions for a_1, a_2, a_3:

$$a_1 \approx C_L^\alpha - \frac{m_z^{\omega z} + m_z^{\dot\alpha}}{r_z^2},$$
$$a_2 \approx -\frac{\mu m_z^\alpha + C_L^\alpha m_z^{\omega z}}{r_z^2},$$
$$a_3 \approx -2C_L^2 \frac{m_z^{\dot\alpha}}{r_z^2} - 2C_D \frac{\mu m_z^\alpha}{r_z^2}.$$

Now the requirement of $a_2 > 0$ is well known condition

$$m_z^{C_L} + \frac{m_z^{\omega z}}{\mu} > 0.$$

For the aircraft investigated the second term is not as low as for the larger aircraft. For $\mu = 1.7$ it is much more higher than the first summand.

In expression for a_1 the first term occurs smaller than the second. From this, one can see that with the changing of the r_z all coefficients a_i change nearly proportionally, so one can obtain rather little information changing r_z.

The next question is the ability to separate the disturbed motion onto short-periodic and long-periodic. One of the ways of roots obtaining described in [2] assumes that there are two pairs of complex conjugated roots, and one pair is much enough comparing to the other with respect to the imagine parts (oscillation frequencies). So, one can obtain the larger roots (in absolute value) from the equation

$$\lambda^2 + a_1\lambda + a_2 = 0$$

and the smaller roots from equation

$$a_2\lambda^2 + a_3\lambda + a_4 = 0.$$

If these roots are really differ significantly, so it is possible to investigate short-period and long-period disturbance separately. The solution of second order equation is well known, so

$$\lambda_{1,2} = \frac{-a_1 \pm i\sqrt{4a_2 - a_1}}{2}, \quad \lambda_{3,4} = \frac{-a_3 \pm i\sqrt{4a_2a_4 - a_3^2}}{2a_2}.$$

3.3 Lateral Motion

Usually [2] the lateral motion is analyzed in the coordinate system in which OX axis is oriented along the wing chord of airplane, OY axis is perpendicular to OX and lies in the symmetry plane of aircraft and OZ axis is perpendicular to OX and OY (and oriented along the wing length).

The necessary relationships required for lateral motion analysis in the coordinate system defined above are represented below.

If β is sideslip angle, then for the wing moment characteristics are [2]

$$\begin{aligned} {m_x}^{\beta}{}_W &\approx -0.5C_L^{\alpha}\bar{z}\cos^2(\chi)\psi - 0.5\bar{z}\sin(\chi)C_L, \\ {m_y}^{\beta}{}_W &= -0.06C_L^2\mathrm{tg}(\chi) - \alpha {m_x}^{\beta}{}_W, \end{aligned}$$

where $\bar{z}$ is the distance from OX axis to the "semi-wing center of gravity" with respect to semi-wingspan, $0.33 < \bar{z} < 0.5$, χ — wing sweep angle, ψ — wing dihedral.

Torque coefficients due to the rotation for the wing are [2]

$$\begin{aligned} {m_x}^{\omega x}{}_W &= -\frac{\xi}{2}\left(2C_L\alpha + k_iC_L^{\alpha}\right), \\ {m_x}^{\omega y}{}_W &= -\frac{\xi}{2}(2 - k_i)C_L, \\ {m_y}^{\omega x}{}_W &= -\xi\left(\left(C_D - C_L\alpha\right)\alpha + C_L\left(\frac{C_L^{\alpha}}{\pi\lambda} - 1\right)k_i\right), \\ {m_y}^{\omega y}{}_W &= -\xi\left(\left(C_D - C_L\alpha\right) - C_L\left(\frac{C_L^{\alpha}}{\pi\lambda} - 1\right)\alpha k_i\right), \\ k_i &= 0.9(0.5 + 0.033\lambda), \end{aligned}$$

where ξ is inertia radius in second power of semi-wing from the symmetry axis with respect to semi-wingspan, $0.33 < \xi < 0.5$.

For the vertical tail

$$
\begin{aligned}
{m_x}^{\beta}{}_T &= k\frac{S_T y_T}{SL}{C_Z}^{\beta}{}_T, \\
{m_y}^{\beta}{}_T &= k\frac{S_T L_T}{SL}{C_Z}^{\beta}{}_T, \\
{m_x}^{\omega x}{}_T &= 2k\frac{S_T}{S}\left(\frac{y_T}{L}\right)^2{C_Z}^{\beta}{}_T, \\
{m_y}^{\omega x}{}_T &= 2k\frac{S_T}{S}\frac{y_T}{L}\frac{L_T}{L}{C_Z}^{\beta}{}_T, \\
{m_x}^{\omega y}{}_T &= 2k\frac{S_T}{S}\frac{y_T}{L}\frac{L_T}{L}{C_Z}^{\beta}{}_T, \\
{m_y}^{\omega y}{}_T &= 2k\frac{S_T}{S}\left(\frac{L_T}{L}\right)^2{C_Z}^{\beta}{}_T, \\
C_{Z}{}_T^{\beta} &< 0
\end{aligned}
$$

where S_T — vertical tail area, y_T — location of vertical tail aerodynamic center along the axis OY, L_T — location of vertical tail aerodynamic center from the center of gravity, k — flow decrease coefficients on the vertical tail.

For further investigations the characteristic “lateral” scale of time

$$\tau_{\perp} = \frac{m}{\rho S V_0}$$

is required.

Dimensionless radii of inertia are

$$r_{XX} = \frac{4I_{XX}}{mL^2}, \quad r_{YY} = \frac{4I_{YY}}{mL^2}$$

where I_{XX} and I_{YY} are inertia moments of airplane about the axes OX and OY. It is assumed that $I_{XY} = 0$.

All torque coefficients below are normalized (assumed to be divided on the appropriate dimensionless inertia radii):

$$\bar{m}_i^q = \frac{m_i^q}{r_{ii}}.$$

With the help of the above relationships the characteristical values λ of dimensionless disturbed motion for level flight can be found from the characteristic equation [2]

$$\lambda^4 + a_1\lambda^3 + a_2\lambda^2 + a_3\lambda + a_4 = 0$$

where [2]

$$
\begin{aligned}
a_1 &= -\left(0.5C_Z^{\beta} + \bar{m}_x^{\omega x} + \bar{m}_y^{\omega y}\right), \\
a_2 &= 0.5C_Z^{\beta}(\bar{m}_x^{\omega x} + \bar{m}_y^{\omega y}) + (\bar{m}_x^{\omega x}\bar{m}_y^{\omega y} - \bar{m}_x^{\omega y}\bar{m}_y^{\omega x}) - \mu(\bar{m}_y^{\beta} + \bar{m}_x^{\beta}), \\
a_3 &= -(0.5C_Z^{\beta}(\bar{m}_x^{\omega x}\bar{m}_y^{\omega y} - \bar{m}_x^{\omega y}\bar{m}_y^{\omega x}) + \mu(\bar{m}_x^{\beta}\bar{m}_y^{\omega x} - \bar{m}_y^{\beta}\bar{m}_x^{\omega x}) - \\
&\quad - \mu\alpha(\bar{m}_x^{\beta}\bar{m}_y^{\omega y} - \bar{m}_y^{\beta}\bar{m}_x^{\omega y}) + 0.5\mu C_L\bar{m}_x^{\beta}), \\
a_4 &= 0.5\mu C_L(\bar{m}_x^{\beta}\bar{m}_y^{\omega y} - \bar{m}_y^{\beta}\bar{m}_x^{\omega y}), \\
C_Z^{\beta} &= {C_Z}^{\beta}{}_T S_T/S_W.
\end{aligned}
$$

For the most part of cases two roots of the characeristical equation are real and two others are complex conjugate values (these roots are responsible for so-called "Dutch step").

Preliminary calculations show that not all the coefficients a_i change proportionally to each other with radii of inertia change. So, changing the inertia radii one can separate the influence of aerodynamical effects and inertia effects.

4 Theoretical and Experimental Results

Above formulas enable to obtain the values of λ_i from the characteristic equations for longitudinal and lateral motion. Also it is possible to obtain these values from experimental data. So, one can compare the reaults and make the conclusion about the applicability the well-known formulas to the case of low Reynolds numbers.

On the basis of data for the model airplane PROGRESS the inertia moments and dimensionless coefficients for this aircraft were obtained.

For the longitudinal motion the following coefficients were obtained: $a_1 = 14.4$, $a_2 = 23.1$, $a_3 = 2$, $a_4 = 0.0037$.

From these data one can obtain that all the roots of characteristic equation are real and all of them are negative. It means that the aircraft is stable in lateral motion. The values of roots are $\lambda_1 = -12.53$, $\lambda_2 = -1.84$, $\lambda_3 = -0.085$, $\lambda_4 = -0.0019$.

Characteristical time is $\tau \approx 0.47$ seconds.

First of all, one can see that the roots form two pairs. One pair are the roots with high values, the other is pair with small values. So, at least for this case it is possible to separate the disturbed motion onto "short-periodic" and "long-periodic".

The absence of "oscillations" (imagine part of the roots) can be explained by very high damping moment of horizontal tail.

To obtain the experimental data required it is necessary to have a part of flight without control impacts.

Figure 3 shows the record of flight data (pitching angle vs time). There is rather long path with no influence of elevator.

One can see that there is practically no oscillations of disturbed motion (a "little wavy" shape can be due to the atmosphere disturbances) as it was predicted by theoretical results.

The same situation is for lateral motion (see fig. 4).

A set of preliminary experiments was also made with changing the inertia radius. For this purpose two additional masses were placed on the wing tips (you can see these masses in fig. 2).

5 Present situation, future work and lessons learned

For this moment the tuning of autopilot was made that enable to record flight parameters. A set of test flights were made on the experimental airplane with autopilot and the records of flight parameters were obtained.

Theoretical results qualitatively coincide with flight data in first approximation. But for the increasing the accuracy of experiment some additional steps must be made. For example, it can be necessary to make the mode of flight with recording "more automatic".

Also, it can be required to increase the accuracy of theoretical data calculations.

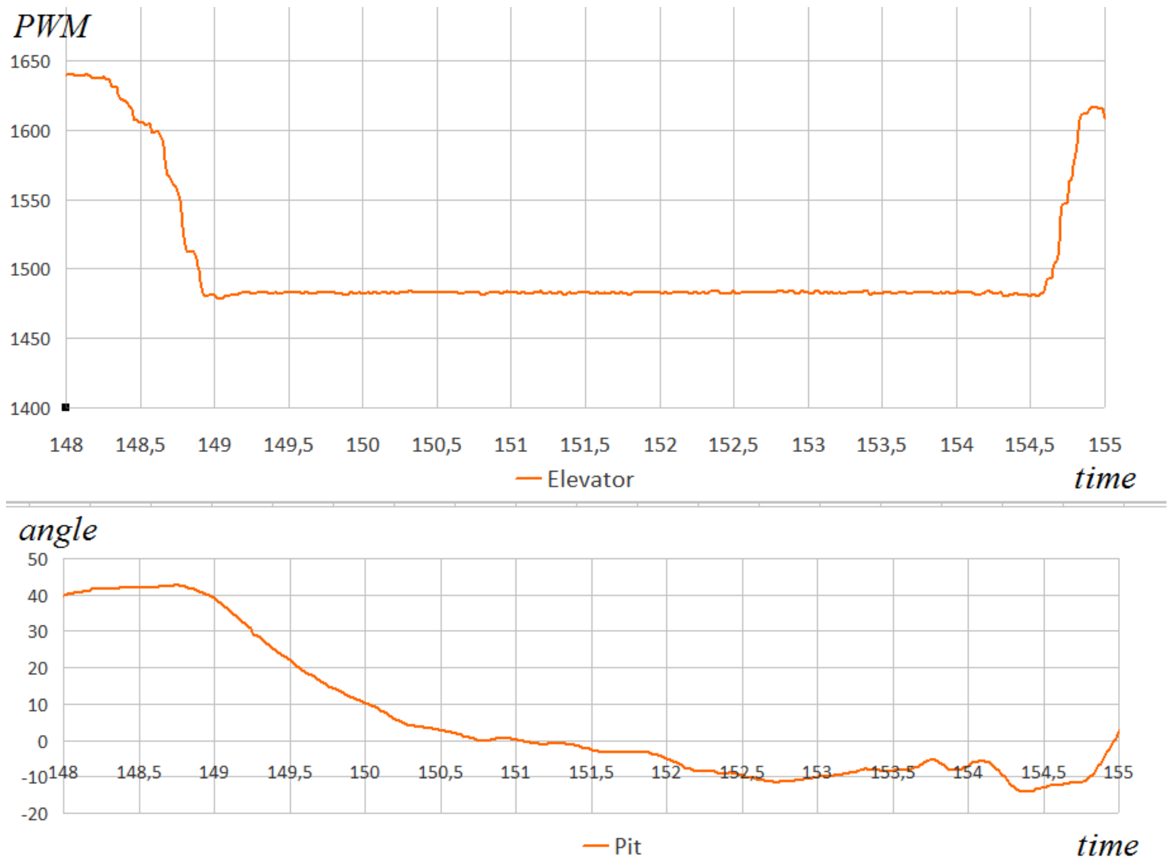

Figure 3: Control signal on elevator (up) and pitch angle (bottom) vs time

Of cause, both experimental and theoretical works must be continued. One more task that must be investigated is the behavior of aircraft at high angles of attack and the steady and unsteady characteristics.

Also the other types of aircrafts (tailless configuration and unconventional configurations) is planned to be investigated.

6 Conclusion

First stage of unsteady MAV characteristics obtaining methodic development with the help of micro autopilot was made. Theoretical data were obtained and a set of flight experiments were made.

Transition from manual to automatic aircraft control is the next step in presented research. This assumes increased accuracy of induced disturbances.

References

[1] Smartap autopilot. [online]. Available at `http://sky-drones.com/`.

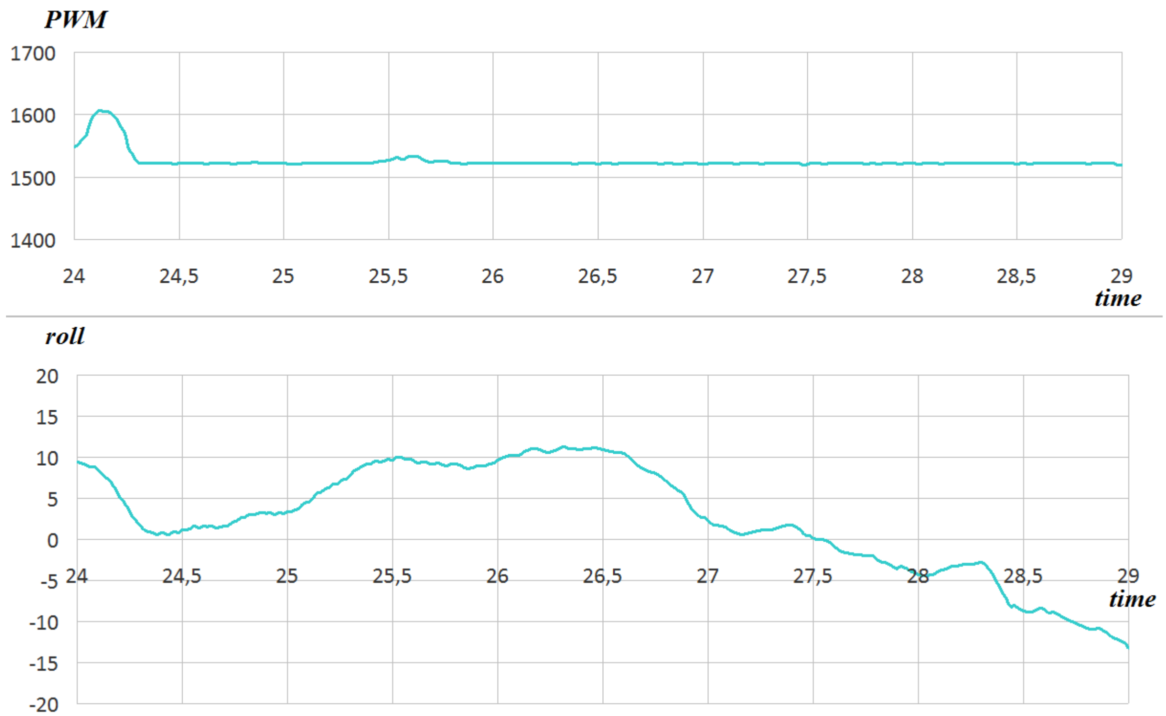

Figure 4: Control signal on aileron (up) and roll angle (bottom) vs time

[2] I. V. Ostoslavsky. *Aircraft Aerodynamics (in Russian)*. Oborongiz, Moscow, 1957.

[3] Kirill Shilov and Grigory Lazurin. MAV autopilot for commercial and research purposes. In *Proceedings of the Conference IMAV 2012*, Braunschweig, Germany, 3-6 July 2012.

[4] Guy Varneuil. Progress sans stress! *Fly International*, (202), January 2012.